

II. Temperature trends in the properties of simple monohydric alcohols. Molecular dynamics simulations of united atom UAMI-EW model*

M. Aguilar ¹, E. Núñez-Rojas ², O. Pizio ¹ †

¹ Instituto de de Química, Universidad Nacional Autónoma de México, Circuito Exterior, 04510, Cd. Mx., México

² Departamento de Química, Universidad Autónoma Metropolitana-Iztapalapa, Av. San Rafael Atlixco 186, Col. Vicentina, 09340, Cd. Mx., México,

Received 11 January 2026; accepted 05 February 2026; published 30 March 2026

We explore the dependence of a wide set of properties of monohydric alcohols on temperature by using the isobaric-isothermal molecular dynamics computer simulations. Namely, methanol (MeOH), ethanol (EtOH) and 1-propanol (PrOH) alcohols are studied. The recently proposed united atom, non-polarizable force field for each of alcohols [V. García-Melgarejo et al., J. Mol. Liq., 2021, **323**, 114576] is applied for this purpose. Accuracy of the force field is discussed comparing predictions from simulations and experimental data for density, dielectric constant, surface tension, and self-diffusion coefficient. Supplementary insights concerning applicability of the model are obtained by exploration of the composition dependence of various properties for MeOH–PrOH mixtures. Peculiarities of mixing of species in this system are elucidated in terms of density, excess mixing volume and excess mixing enthalpy. Static dielectric constant of the mixture and the corresponding excess are obtained. Perspectives of modelling are commented finally.

Key words: *methanol, ethanol, 1-propanol, temperature dependence, molecular dynamics simulations*

1. Introduction

Theoretical modelling of alcohols and their mixtures with water and other substances is of much importance for chemical engineering. This topic generated enormous amount of studies using experiments, computer simulations and semi-analytical constructions. In spite of much efforts, the problem of describing the properties of these systems at different pressures, temperatures and chemical composition (in the case of multi-component mixtures) is far from being solved. Even for rather simple molecular fluids, such as lower alcohols, and their mixtures, the current understanding of the trends of behavior of principal properties regarding thermodynamic conditions is not complete [1, 2].

One of the most frequently used and accurate united-atom models for simple alcohols is provided by the TraPPE database [3]. The coexisting vapor-liquid density, boiling temperature, vapor pressure and critical properties are used to derive parameters of the force field. On the other hand, the UAMI model with explicit water, denoted as UAMI-EW united atom, non-polarizable model for different monohydric alcohols was constructed by considering the density, the static dielectric constant and surface tension as targets [4]. In contrast to TraPPE united atom modelling, the UAMI-EW force field leads to correct miscibility values for lower alcohols with water as documented in [4]. This scheme of parametrization was designed at a room temperature, 298.15 K, and ambient pressure, 1 bar, thermodynamic state. It is worth noting that the TIP4P/ε water model is involved within applied parametrization.

The principal objective of the present work is to investigate the temperature dependence of a set of properties of simple monohydric alcohols (MeOH, EtOH and PrOH) by using the UAMI-EW united

*Dedicated to the memory of Prof. Stefan Sokolowski

†Corresponding author: oapizio@gmail.com

atom, non-polarizable models. Very recently, we have tested these models with respect of its applicability at a fixed temperature, 298.15 K, but in a wide interval of pressure values [5, 6]. Namely, in reference [5] we explored the evolution of the principal properties of the UAMI-EW model from ambient pressure, 1 bar, up to 3 kbar, for each of three alcohols in question. We refer to this reference as part I below. On the other hand, in reference [6], the main objective was to elucidate the trends of behavior of the hydrogen bonds network of UAMI-EW united atom model for methanol, along with other popular methanol models [3, 7], up to high pressure, 6 kbar. It is well established that water molecules form a three dimensional network of tetrahedrally coordinated molecules, see, e.g., references [8, 9], whereas in liquid methanol chains and/or branched chains can be detected. This leads to well pronounced differences of the topology of the hydrogen bonds network in aqueous alcohol solutions in comparison with pure alcohols [10, 11].

The second part of the present work is devoted to the study of MeOH–PrOH mixtures at different temperatures. In this way we would like to elucidate the applicability of the present UAMI-EW modelling to alcohol mixtures. In future work from our laboratory, this investigation will be extended to secondary alcohols in the spirit of the previous, quite recent studies [1, 2].

2. Models and simulation details

In general terms, within this type of modelling, the interaction potential between all atoms and/or groups is assumed as the sum of Lennard-Jones (LJ) and Coulomb contributions. Lorentz–Berthelot combination rules are used to determine the cross parameters for the relevant potential well depths and diameters.

Molecular dynamics computer simulations of water-methanol mixtures were performed in the isothermal–isobaric (NPT) ensemble at a given pressure and temperature. We used GROMACS software [12] version 5.1.2. The simulation box in each run was cubic, the number of molecules of the species in all cases was fixed at 3000. Periodic boundary conditions were used. Temperature and pressure controls were provided by the application of V-rescale thermostat and Parrinello–Rahman barostat with $\tau_T = 0.5$ ps and $\tau_P = 2.0$ ps, respectively, the timestep was 0.002 ps. The compressibility value $4.5 \times 10^{-5} \text{ bar}^{-1}$ was used.

The non-bonded interactions were cut-off at 1.1 nm, whereas the long-range electrostatic interactions were handled by the particle mesh Ewald method (fourth order, Fourier spacing equal to 0.12) with the precision 10^{-5} . The van der Waals correction terms to the energy and pressure were applied. In order to maintain the geometry of alcohol intra-molecular bonds rigid, the LINCS algorithm was used. All the parameters for the force fields are given in the supplementary material to reference [4].

After preprocessing and equilibration, consecutive simulation runs, each with time duration not less than 10 ns, with the starting configuration being the last configuration from the previous run, were performed to obtain the trajectories for the data analysis. The results for the majority of properties were obtained by averaging over 7–10 production runs. The dielectric constant and self-diffusion coefficients were evaluated from the entire trajectory.

3. Results: MeOH, EtOH and PrOH alcohols

Each of the properties below is considered for three alcohols, MeOH, EtOH and PrOH, in order to capture the effect of length of the hydrophobic part of alcohol molecule. In the majority of cases we intended to cover the entire interval of temperatures where the experimental data are available.

3.1. Density

We begin with the dependence of density for each of alcohols on temperature at ambient pressure, 1 bar. The corresponding lines are shown in three panels of figure 1. The simulation results for UAMI-EW model are given by red lines decorated by solid squares. Another notation is explained in the figure caption. We observe that the model in question provides a quite good description of density on

temperature as it follows from comparison with experimental data. The accuracy of the model is better for MeOH and EtOH compared to PrOH. Nevertheless, even in this case, the deviation of simulation data from experimental points is very small in percentage.

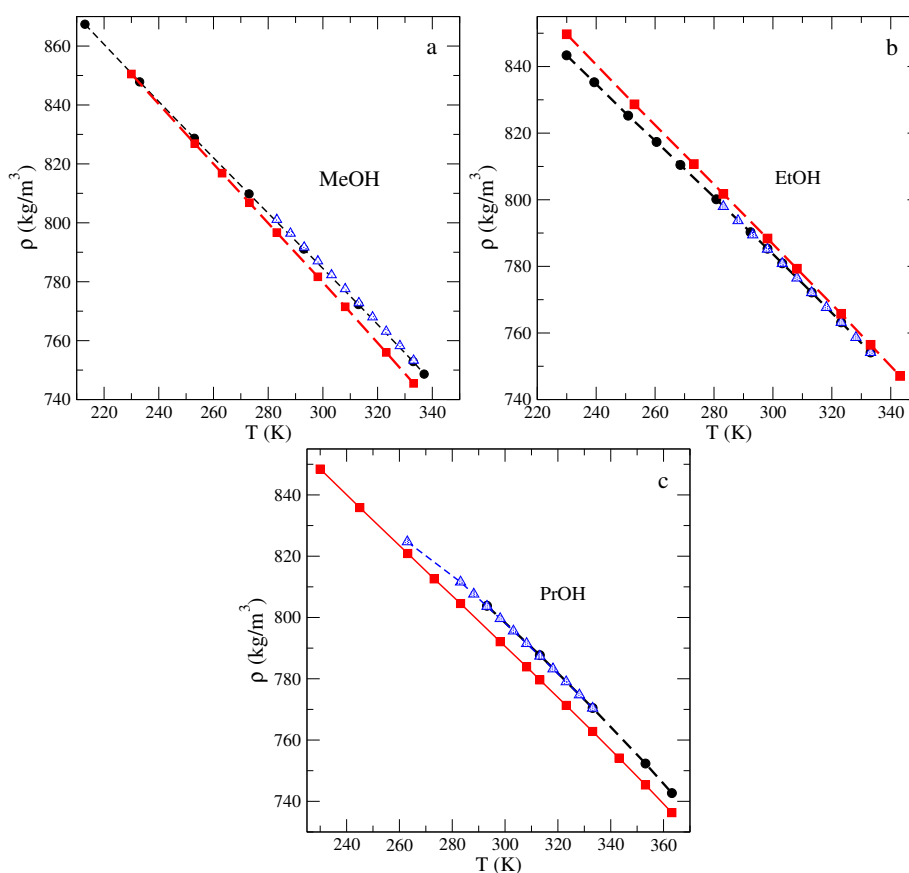


Figure 1. (Colour online) Panel a: methanol density on temperature at pressure 1 bar. The experimental data (black short-dashed line and solid circles) are from NIST Chemistry Webbook [13] and from reference [14] (blue hollow triangles). Panel b: ethanol density on temperature. The experimental data are from: Sun et al. [15] (black circles) and reference [14] (blue hollow triangles). Panel c: experimental data from [16] (black circles), [14] (blue hollow triangles). Our simulation data of UAM-EW model are given by red dashed line with solid squares in all panels.

We would like to recall that the dependence of density on pressure at room temperature, 298.15 K, for each of alcohols in question is described rather well, cf. figure 1 of reference [5]. Thus, concerning volumetric properties determined mainly by density, the UAMI-EW model can be used in a large portion of T, P plane with sufficient confidence.

3.2. Dielectric constant

The dielectric constant is one of the most important physico-chemical properties of a given liquid, since to much extent it determines the properties of mixing with other substances. The static dielectric constant has served as a target property in the parametrization of UAMI-EW model at $T = 298.25$ K and $P = 1$ bar, besides the density and surface tension. Our results for ε at different temperatures follow from the time-average of the fluctuations of the total dipole moment of the system as common [17],

$$\varepsilon = 1 + \frac{4\pi}{3k_B T V} (\langle \mathbf{M}^2 \rangle - \langle \mathbf{M} \rangle^2), \quad (3.1)$$

where k_B is the Boltzmann constant and V is the simulation cell volume.

All the results for three alcohols, MeOH, EtOH and PrOH, are given in panels a, c and d of figure 2. We keep the same nomenclature for simulation results (red lines with solid squares) for the sake of convenience of the reader. In panel b, the time dependence of the value for the dielectric constant for MeOH is illustrated. The density of each alcohol increases upon decreasing temperature (cf. figure 1), apparently longer in time trajectories are necessary to reach the plateau that determines the value for ϵ . We observe that the model for MeOH slightly underestimates the dielectric constant in comparison with experiment (figure 2a). At low temperatures, the deviation of simulations results from experiments becomes larger, in comparison with high temperatures where thermal fluctuations are stronger. For alcohols with longer hydrophobic part of the molecule, the agreement between simulation results and experimental data is satisfactory. Hence, parametrization of the model at $T = 298.15$ K, provides a reasonable description of the static dielectric constant in a quite large interval of temperature changes. This conclusion may be considered together with the findings for $\epsilon(P)$, cf. figure 4 of reference [5]. Both of them support a successful applicability of UAMI-EW model for the description of dielectric constant of each of three alcohols in question in the T, P plane. One of the missing elements, or say possible extension necessary to complete, is in the study of dielectric relaxation phenomena for alcohols with a different number of carbon groups in the hydrophobic part of the molecule. We hope to address this issue in our future work.

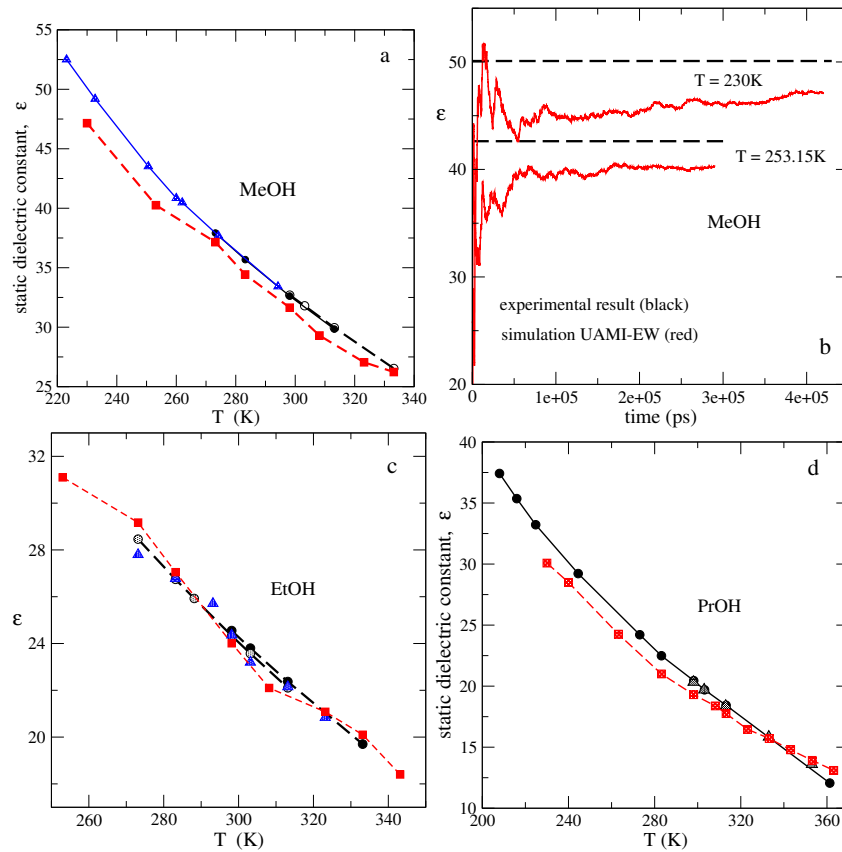


Figure 2. (Colour online) Panel a: dielectric constant of methanol on temperature. The experimental data in panel a are from reference [18] (black solid circles), [19] (hollow circles), [20] (blue triangles). The simulation results (red squares in panels a, c and d) are for UAMI-EW united atom model. Panel b: illustration of the calculations of dielectric constant of methanol. Panel c: experimental data are from reference [19] (black solid circles), [18] (shaded circles), [21] (blue triangles), respectively. Panel d: experimental data are from references [21] (black circles) and [19] (triangles), respectively.

3.3. Surface tension

We proceed now to the surface tension, γ , on temperature trends. This property was used as one of the targets in the construction of UAMI-EW model. The entire set of results obtained is given in figure 3.

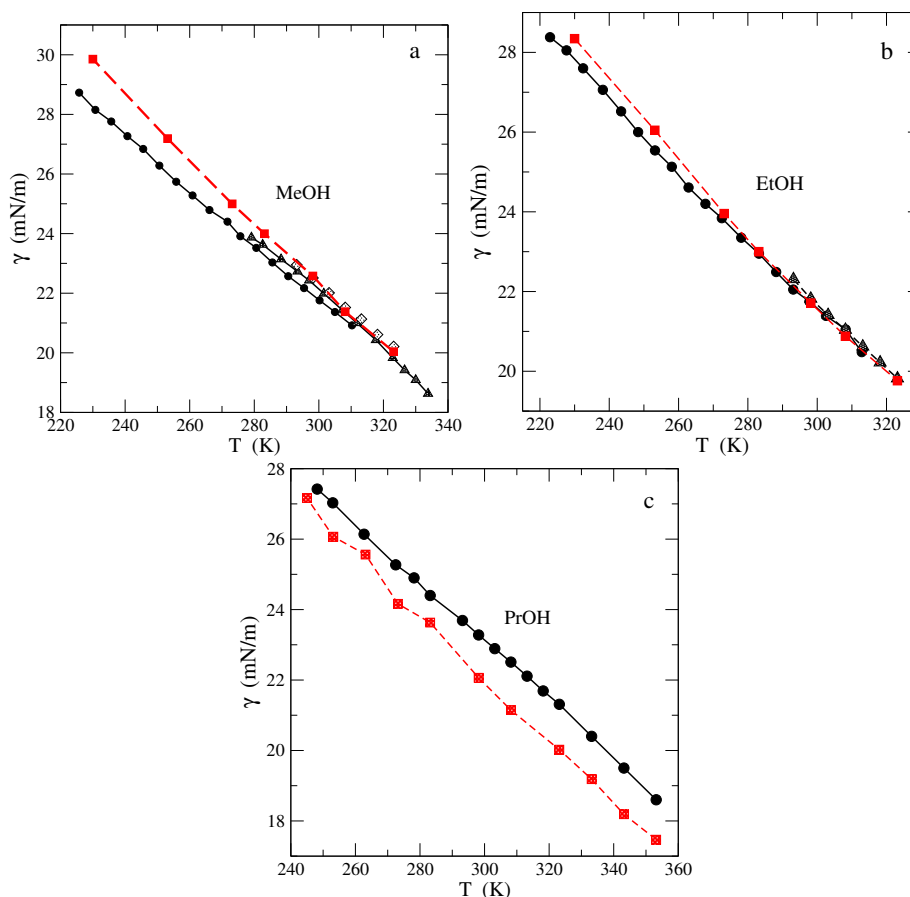


Figure 3. (Colour online) Panel a: surface tension of methanol on temperature. The experimental data in panel a are from reference [22] (circles), [23] (triangles) and [24] (diamonds), respectively. Panels b and c: the same as in panel a, but for EtOH and PrOH, respectively. Experimental data are from reference [22] (circles — in panels b and c) and from [24] (triangles) in panel b. The simulation results in all panels are for UAMI-EW united atom model (squares).

In general terms, the UAMI-EW model correctly describes $\gamma(T)$ dependencies for each of three alcohols. An overall agreement between simulation results and experimental data is observed. This agreement is better for MeOH and EtOH (panels a and b). Nevertheless, at low temperatures, the UAMI-EW model overestimates the surface tension values, in comparison with experimental results. On the other hand, for PrOH, the model underestimates the values for the surface tension in the entire temperature interval under study (panel c). The absolute value of deviation of simulation results from experiment is around 5%. This behavior reflects the impossibility to reproduce several properties simultaneously with high precision at the level of united atom modelling. Still, the optimum balance of accuracy with small margins for a set of properties can be reached.

We have evaluated the density profiles of alcohol molecules across liquid–vapor interface, but do not show them for the sake of brevity. It may be of interest to discuss them more in detail in a separate publication.

3.4. Self-diffusion coefficient

Evaluation of the quality of the model often involves results for the self-diffusion coefficient, D . Note that D was not considered as a target property within the multi-step parametrization of the UAMI-EW model [4].

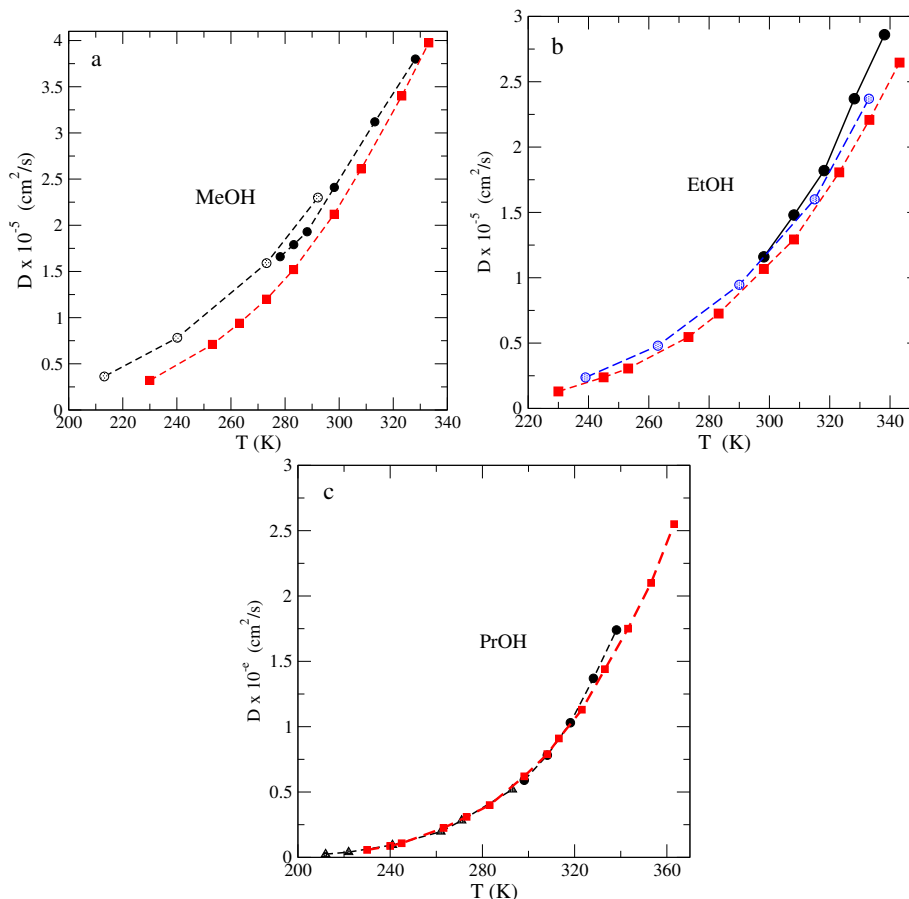


Figure 4. (Colour online) Panel a: self-diffusion coefficient of methanol on temperature. Experimental data are from [25, 26] (solid circles), and [26] (hollow circles). Panel b: self diffusion coefficient of ethanol on temperature (experimental data — [27], [26], solid and hollow circles, respectively). Panel c: self diffusion coefficient of PrOH on temperature (experimental data — [27, 28], circles and triangles, respectively).

One of the common routes to obtain D , is from the mean square displacement of particles. On the other hand, it may be also calculated from the velocity auto-correlation function. We calculate D by the former method, via the Einstein relation,

$$D = \frac{1}{6} \lim_{t \rightarrow \infty} \frac{d}{dt} |\mathbf{r}(\tau + t) - \mathbf{r}(\tau)|^2, \quad (3.2)$$

where τ denotes the time origin. Default settings of GROMACS were used for the separation of the time origins.

The dependence of D on temperature from simulations of three alcohols in question is shown in figure 4. Besides, the figure contains available experimental data for sake of comparison. It can be seen that D increases with increasing temperature for each alcohol, in agreement with the trends of experimental data. Thermal movement facilitates self-diffusion, as expected. The values of D for MeOH from simulations are underestimated over the entire temperature range compared with the experimental results. On the other hand, the agreement between simulations and experiments is very good for EtOH

and PrOH. The temperature interval is limited from above by the boiling temperature for each alcohol. At low temperatures, we have not attempted to explore the behavior of self-diffusion coefficient very close to solidification. Having in mind a satisfactory performance of the UAMI-EW force field for $D(P)$ at $T = 298.15$ K, cf. figure 5 of reference [5], we would just like to note that the model provides a successful description of the self-diffusion coefficient for liquid alcohols under study in the (T, P) -plane. More extensive insights into the dynamic properties can be obtained by performing additional simulations and analysis of the resulting different auto-correlation functions.

On the other hand, it is worth to comment that certain insights into the structural properties of primary alcohols within UAMI-EW model were discussed in the recent work from this laboratory [29]. Principally, they refer, however, to various distribution functions and coordination numbers of alcohol–water mixtures. For pure alcohols, our very recent research on the microscopic structure restricted to the behavior of methanol solely, in a quite wide interval of values for pressure [6]. A reasonable agreement of the structural properties of methanol model, in comparison with the X-ray and neutron scattering results for the structure factors, was obtained. Moreover, cooperative effects of the hydrogen bonds network in MeOH were elucidated. We expect that progress in the structure measurements for other primary alcohols at different pressures and temperatures will be reached soon, and will make possible a comparison of simulation results for the structure and experimental data.

Natural extension of the modelling of alcohols explored above is in its application to mixtures. Specifically, we would like to investigate whether the level of accuracy of the results for pure alcohols is sufficient to provide appropriate and correct trends of the behavior for their mixing properties.

4. Application of the UAMI-EW model to MeOH–PrOH mixtures

Most frequent and abundant simulations were performed for mixtures of simple primary alcohols with water. On the other hand, several studies were focused on the description of mixing properties of various alcohol binary mixtures. We refer to references [1, 2] as illustrative examples. These systems are of much importance for practical applications.

Sophistication of the models for single-component alcohols, starting from the united atom description [3, 4] up to all-atom [30] and polarizable models, see, e.g., [31], resulted in their application for binary mixtures of primary alcohols. Namely, we found and refer here to some of the results coming from all-atom modelling [32] and of ab initio modelling [33]. These two works from the same laboratory intended to elucidate a few principal features of the behavior of binary alcohol mixtures. Thus, we decided to explore the mixing properties of MeOH and PrOH and extend the evaluation of accuracy of UAMI-EW modelling. It is worth mentioning that binary alcohol mixtures are much less studied experimentally, in comparison with alcohol–water solutions. Some of experimental observations, however, challenge computer simulations modelling. Namely, as documented in reference [2], temperature dependence of mixing enthalpy for mixtures of primary and secondary alcohols exhibits peculiarities that require appropriate modelling.

To begin with, a comparison of our simulation data for the composition dependence of density of MeOH–PrOH solutions with experimental results at different temperature values, is shown in figure 5. It is worth noting that a set of experimental density values from reference [34] in figure 5a includes solely five points at each of temperatures, $T = 293.15$ K and $T = 333.15$ K, in contrast to a more detailed measurements at $T = 298.15$ K from [35]. This work [34] is focused on the study of shear viscosity, rather than on the precise evaluation of density. Moreover, the experimental point at $X_{\text{MeOH}} = 0.755$, is a bit out of trend, as it can be seen from the lines in figure 5a. The density of mixtures under study smoothly decreases from the value for pure PrOH to pure MeOH exhibiting a weak non-linearity at each temperature considered.

In general terms, we observe that the UAMI-EW model underestimates the values for density in the entire interval of composition for three temperatures studied, panels a and b of figure 5. However, the magnitude of discrepancy of simulation results compared to experimental values is of the order of 1%. Moreover, the shape of $\rho(X_{\text{MeOH}})$ dependence from simulations agrees well with experimental trends of behavior of this property.

In figure 5b, we added the curve (reproduced from reference [32]) describing the simulation results

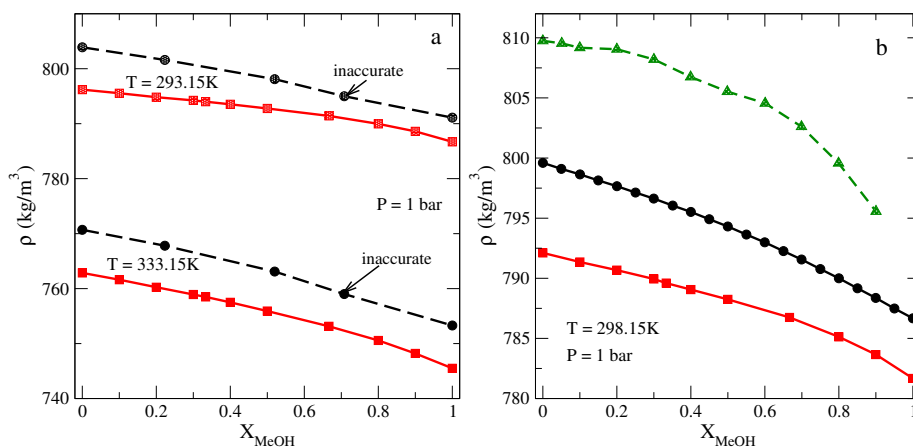


Figure 5. (Colour online) Panel a: a comparison of simulation data (red squares) for the composition dependence of density for MeOH–PrOH mixture with experimental data (circles) from [34]. Panel b: density of MeOH–PrOH mixture on composition from simulations, and experimental data [35], nomenclature of symbols as in panel a, green triangles reproduced from figure 1a of reference [32] — simulation of OPLS/AA model.

using the all-atom, OPLS/AA, model for both alcohol species. The shape of this curve differs from the experimental trend, its non-linearity is overestimated in comparison with the experimental data. Moreover, at low and intermediate methanol concentration, the magnitude of deviation from experimental results is larger compared with the UAMI-EW united atom model.

Trends of behavior of density upon changes of composition can be interpreted in terms of the mixing properties. Specifically, in figure 6 we plot the dependence of the excess mixing volume, $\Delta V_{\text{mix}}^{(ex)} = V_{\text{mix}} - X_{\text{MeOH}}V_{\text{MeOH}} - (1 - X_{\text{MeOH}})V_{\text{PrOH}}$, on X_{MeOH} at different temperatures.

In order to gain confidence about the trends of behavior of $\Delta V_{\text{mix}}^{(ex)}$ versus X_{MeOH} upon temperature change from $T = 298.15$ K to $T = 333.15$ K for a binary alcohol system, we performed additional simulations for MeOH–water and PrOH–water mixtures at $T = 298.15$ K and $T = 323.15$ K because the experimental data at these conditions are available. The results are shown in figures 6a and 6b. The experimental data witness that the maximum absolute value for $\Delta V_{\text{mix}}^{(ex)}$ increases for MeOH–water mixture upon the temperature change from 298.15 K to 323.15 K (figure 6a). By contrast, opposite behavior is observed for PrOH–water system (figure 6b) within the same temperature interval. The UAMI-EW model for each of two alcohols combined with the TIP4P/ε model for water reproduce this behavior qualitatively correctly. If both alcohols are modelled within the UAMI-EW model, the excess mixing volume for MeOH–PrOH system behaves as shown in figure 6c. Two, statistically significant sets of independent experimental data, at $T = 298.15$ K, confirm that $\Delta V_{\text{mix}}^{(ex)}$ reaches the maximum value at $X_{\text{MeOH}} \approx 0.6$. The absolute value for $\Delta V_{\text{mix}}^{(ex)}$ at this particular composition and within the entire composition range is small, as expected for nearly ideal behavior of two mixed, quite similar, species. The data set from reference [39] predicts negative values for $\Delta V_{\text{mix}}^{(ex)}$ at $X_{\text{MeOH}} \approx 0.95$ (i.e., for systems with very small amount of 1-propanol dissolved in MeOH), in contrast to dataset from [38] that indicates positive $\Delta V_{\text{mix}}^{(ex)}$ in the entire composition range.

The simulation results for UAMI-EW model deviate from the experimental data, except for the composition interval corresponding to propanol-rich mixtures. Hence, the model is not highly accurate for geometric aspects of mixing of quite similar alcohol species. Actually, the UAMI-EW model overestimates the influence of PrOH component in the $\Delta V_{\text{mix}}^{(ex)}$ dependence on composition, X_{MeOH} .

At $T = 333.15$ K, a comparison of simulation data and experiment is more difficult to perform. The experimental density values from reference [34] in figure 5a include solely five points at 333.15 K. These data can be easily converted into the excess mixing volume values to yield three points only for intermediate X_{MeOH} , see, e.g., equation (2) from reference [40]. Thus, the results do not provide

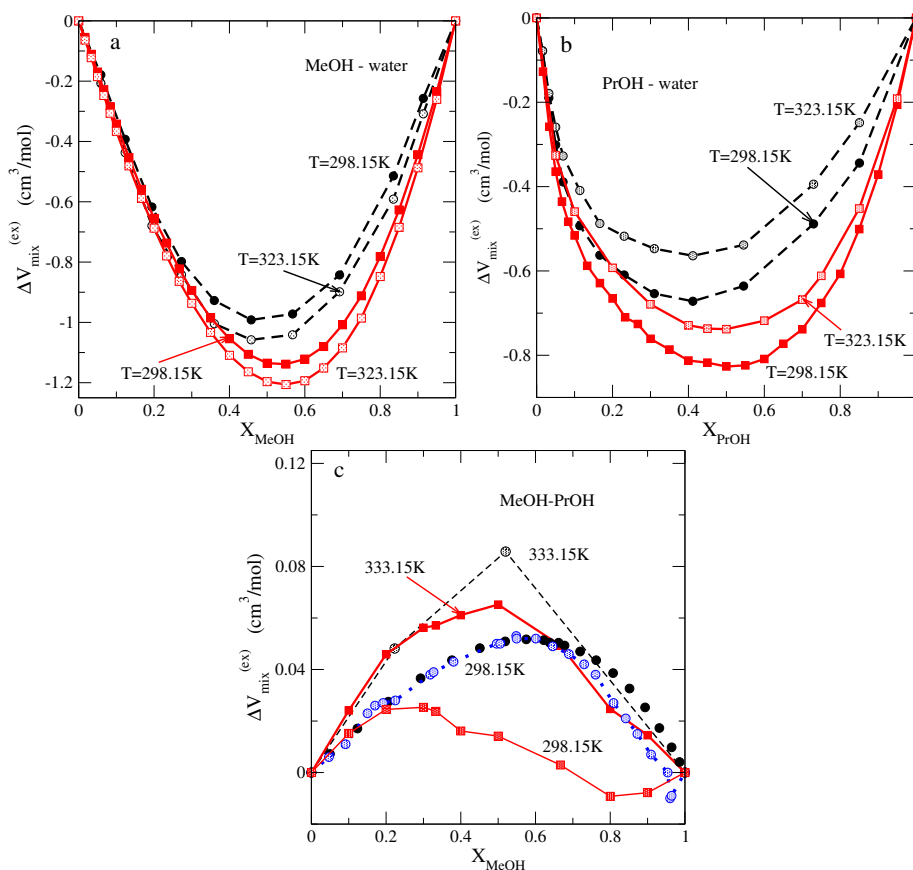


Figure 6. (Colour online) Panels a and b: the excess mixing volume for MeOH–water and PrOH–water mixtures on composition at two values of temperature, respectively. The experimental data (circles) are from Mikhail and Kimmel [36, 37] in both panels, respectively. The simulations are for UAMI-EW model combined with TIP4P/ε model (squares). Panel c: excess mixing volume for MeOH–PrOH mixture on composition. The experimental data are from references [38, 39] at $T = 298.15$ K (black and blue circles, respectively). The simulations are UAMI-EW model for both alcohols at different temperatures (squares). The experimental points at $T = 333.15$ K (shaded circles) were calculated from the density values given by Kumagai [34] (the point at $X_{\text{MeOH}} = 0.755$ has been omitted due to inaccuracy).

statistically significant trends. Nevertheless, we observe that simulations predict positive values for $\Delta V_{\text{mix}}^{(ex)}$ in the entire composition range in accordance with experimental values. In summary, we claim that for binary alcohol mixture in question, the excess mixing volume values increase in magnitude upon increasing temperature. Hence, the observed trend on temperature exhibits similarity to the behavior of PrOH–water mixtures shown in figure 6b. Unfortunately we are not aware of other studies of excess mixing volume for binary alcohol mixtures on temperature.

Let us proceed now to the exploration of energetic aspects of mixing on temperature. To do that, we performed a similar analysis as just above for the excess mixing volume. The excess mixing enthalpy from simulations and experiments is shown in figure 7. A set of results from additional simulations of alcohol–water mixtures is given in panels a and b of figure 7. The behavior of $\Delta H_{\text{mix}}^{(ex)}$ on X_{MeOH} in figure 7a for MeOH–water systems witness exothermic mixing of species. However, the maximum absolute value for $\Delta H_{\text{mix}}^{(ex)}$ decreases upon increasing temperature for MeOH–water mixtures. This case was discussed in our recent publication [43] more in detail.

On the other hand, the dependence of $\Delta H_{\text{mix}}^{(ex)}$ on X_{PrOH} at different temperature values is more complex (figure 7b). The experimental data for $\Delta H_{\text{mix}}^{(ex)}$ at $T = 298.15$ K and $T = 323.15$ K show the

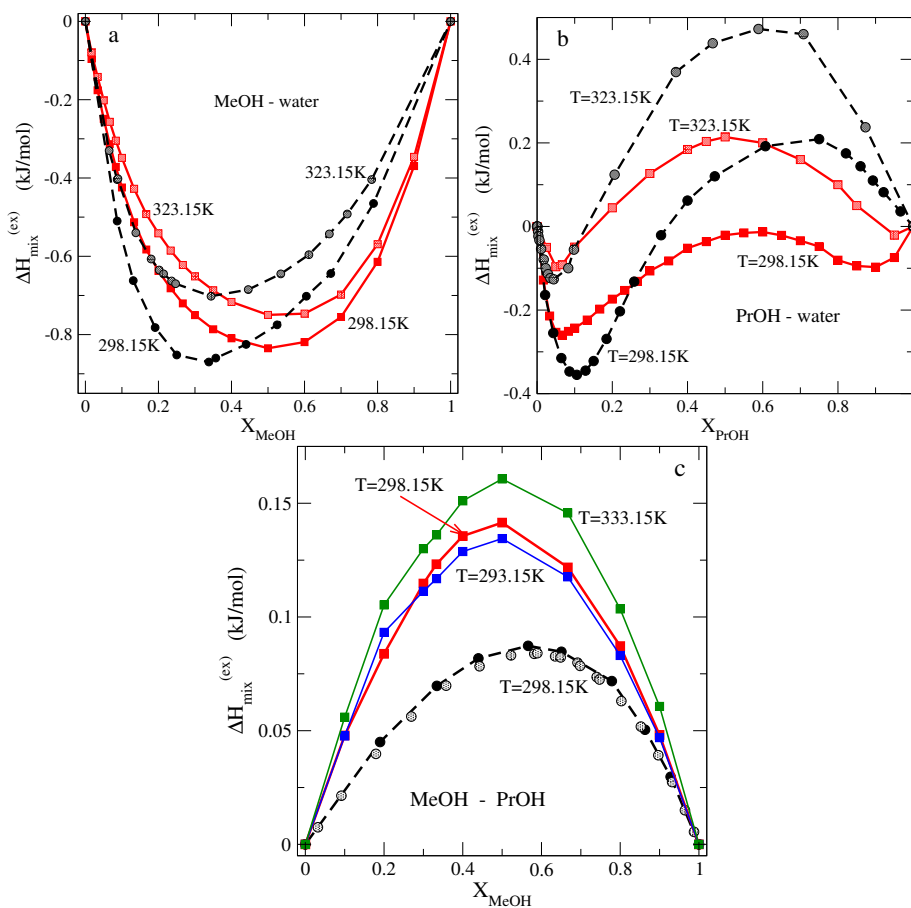


Figure 7. (Colour online) Panels a and b: the excess mixing enthalpy for MeOH–water and PrOH–water mixtures on composition at two values of temperature, respectively. The experimental data in panel a are from reference [41, 42] (solid and shaded black circles, respectively) and from [44, 45] (solid and shaded circles, respectively) in panel b. Panel c: excess mixing enthalpy of methanol–propanol mixture on methanol mole fraction at 298.15 K and 1 bar. Molecular dynamics simulation results of UAMI-EW model (red squares). Experimental results at 298.15 K are from references [46, 47] (solid and shaded black circles, respectively).

presence of a minimum of this function for water-rich mixtures and a maximum for PrOH-rich mixtures. Thus, one observes a transition from exothermic to endothermic mixing behavior at both temperature values. The computer simulation results reproduce temperature trends in agreement with experimental behavior. However, at each temperature, the composition trends are only in a qualitative agreement with experiments. The values for $\Delta H_{\text{mix}}^{(ex)}$ from simulations are better reproduced for water-rich mixtures, figure 7b.

The simulation results for binary alcohol mixtures overestimate the magnitude of values for $\Delta H_{\text{mix}}^{(ex)}$ in the entire interval of compositions, in comparison with experimental data, figure 7c. In general, the absolute values for $\Delta H_{\text{mix}}^{(ex)}$ are smaller for binary alcohol mixture, in comparison with alcohol–water systems, as actually expected. The UAMI-EW model correctly predicts the endothermic mixing behavior. Moreover, it yields the symmetric curve with maximum deviation from ideality at $X_{\text{MeOH}} = 0.5$. The experimental data exhibit maximum at a slightly more prevailing methanol concentration at $T = 298.15$ K. On the other hand, the maximum of $\Delta H_{\text{mix}}^{(ex)}$ from simulations becomes larger at $T = 333.15$ K than at lower temperatures. We are not able to verify the accuracy of temperature trends because the experimental data are restricted to 298.15 K solely.

Concerning the comparison of the present results with findings of other authors, we would like to attract the attention of the reader to the results shown in figure 1a of reference [2]. Apparently, the UAMI-EW model predicts the $\Delta H_{\text{mix}}^{(ex)}(X_{\text{MeOH}})$ dependence a bit better than the TraPPE one. At least, the maximum value for $\Delta H_{\text{mix}}^{(ex)}(X_{\text{MeOH}})$ following from UAMI-EW is closer to the experimental value. It is not known if the UAMI-EW force field in its present form is sufficiently good for primary alcohol–secondary alcohol mixtures. This issue was discussed using TraPPE modelling for the excess mixing enthalpy in reference [2]. For UAMI-EW force field, the problem requires a separate study.

In the recent study of mixtures of primary alcohols and of primary and secondary alcohols, Chang and Siepmann [2] discussed the role of hydrogen bonds in modifying the temperature trends of mixing enthalpy. Apparently, even small changes of the number of hydrogen bonds between molecules may lead to a more pronounced changes in the mixing properties. For the sake of illustration, we show the composition dependence of the average number of bonds per molecule for MeOH–PrOH mixtures in figure 8. This property was obtained by application of the gmx hbond facility with default parameters using GROMACS software.

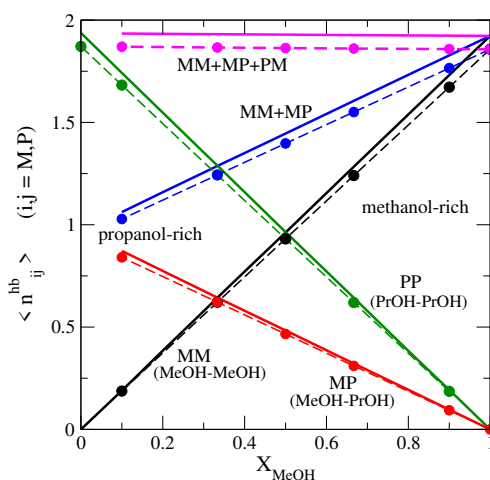


Figure 8. (Colour online) Average number of hydrogen bonds per molecule in methanol–propanol mixture on methanol mole fraction. Molecular dynamics simulation results are for UAMI-EW model for both species. Lines are for $T = 298.15\text{ K}$, whereas the lines decorated with circles are for $T = 333.15\text{ K}$, $P = 1\text{ bar}$.

Each of pure components, MeOH and PrOH, is characterized by a similar value for the average number of bonds per molecule, $n_{MM}^{hb} \approx n_{PP}^{hb} \approx 2$, indicating the dominance of chain-like structure. The lines describing the bonding of species are linear and practically symmetric with respect to equimolar composition. The total number of bonds per molecule of each species is almost constant in the entire interval of composition, as expected for a mixture of very similar species. This behavior is in sharp contrast to the changes observed for hydrogen bonding in methanol–water mixtures upon composition, see detailed discussion of this issue in, e.g., reference [48]. However, the principal conclusion for the system in question, is that quite small changes of bonding due to temperature changes (figure 8) are manifested in a more pronounced changes of the excess mixing enthalpy in figure 7c.

Next, we proceed to the comparison of the dielectric constant and of the excess dielectric constant from our simulations with experimental data from reference [49]. Our results are illustrated in two panels of figure 9. From panel a of this figure we learn that the UAMI-EW model for the MeOH–PrOH mixture pretty well describes the composition behavior of the static dielectric constant, $\varepsilon(X_{\text{MeOH}})$. The model appropriately describes the shape of this function. The deviation between simulation results and experimental data is not big in the entire composition interval. By contrast, the differences between the results of all-atom modelling [32] and experimental ones are much bigger. On the other hand, the results from ab initio modelling [33] also deviate from experimental points. Inaccuracy of the points on the curve $\varepsilon(X_{\text{MeOH}})$ become more pronounced on the line that shows the excess dielectric constant, figure 9b. We

observe that the UAMI-EW model is very successful in describing the $\Delta\epsilon(X_{\text{MeOH}})$ dependence. A small deviation from the experimental predictions is seen on the propanol-rich side. The all-atom modelling and ab initio results are much less successful in the description of $\Delta\epsilon(X_{\text{MeOH}})$ behavior. Unfortunately, we are not aware of the results for the dielectric constant of the system in question at temperatures higher and lower than 298.15 K.

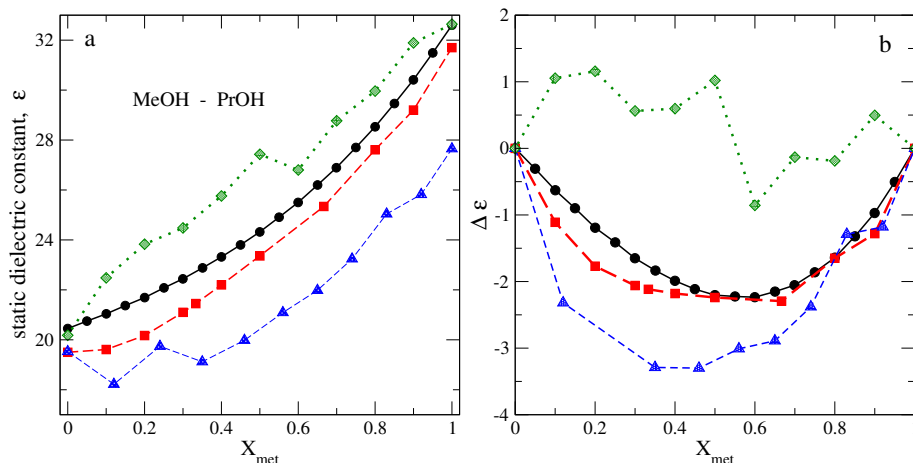


Figure 9. (Colour online) Panel a: dielectric constant of MeOH–PrOH mixture on mixture composition, experiment [49] (black solid circles), simulation — UAMI-EW (red squares), ab initio results reproduced from reference [33] (green diamonds). Blue triangles — simulations of OPLS/AA model reproduced from reference [32]. Panel b: excess dielectric constant on composition. The nomenclature of lines and symbols as in panel a.

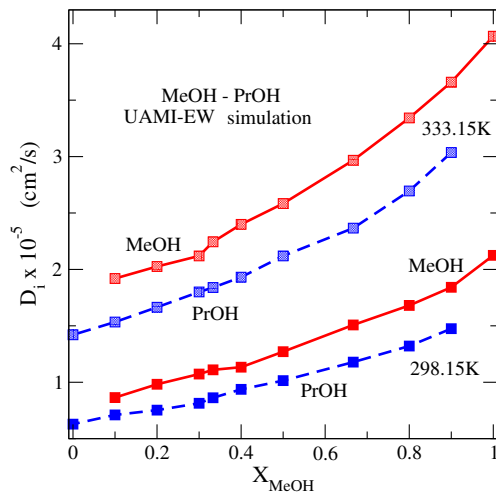


Figure 10. (Colour online) Self-diffusion coefficients of components in methanol–propanol mixture on methanol mole fraction at $T = 298.15$ K and at $T = 333.15$ K, at ambient pressure, 1 bar. Molecular dynamics simulation results for UAMI-EW model.

The final issue of our interest in the present work concerns the composition dependence of the self-diffusion coefficients of species for the mixtures under study, figure 10. It is worth mentioning that self-diffusion coefficients may serve as tests of the force fields and to seek for their improvement. The experimental data for self-diffusion coefficients for binary alcohol mixtures are available for methanol–ethanol mixtures on composition at 298.15 K [50] (note incorrect spelling of the author’s surname,

Uedaira, in the journal web-page, that made tedious our search of the relevant literature). Another set of data for MeOH–EtOH system was published very recently [51]. In spite of an extensive search, we have not found the data for MeOH–PrOH liquid mixture, unfortunately.

Our simulation results for MeOH–PrOH system, show that the values of self-diffusion coefficients, $D_i(X_{\text{MeOH}})$, for each species increase with increasing methanol amount in the mixture. $D_{\text{MeOH}}(X_{\text{MeOH}})$ values are larger than of $D_{\text{PrOH}}(X_{\text{MeOH}})$, i.e., smaller molecules move faster than the bigger ones. As smaller inclination of the curves with concentration of methanol is observed for propanol-rich mixtures. In qualitative terms, the trends of behavior of $D_i(X_{\text{MeOH}})$ shown in figure 10 agree with the experimental observations for MeOH–EtOH mixtures, see, e.g., figure 1 of reference [50] and figure 1 of [51]. There is a small qualitative difference between these two sets of experimental data at a very small methanol concentration that may be attributed to the deuterated sample used in the former study [50]. In summary, we are convinced that the concentration dependence of the self-diffusion coefficients coming from UAMI-EW simulations is captured satisfactorily.

5. Concluding remarks

To conclude, we would like to note that the recently proposed modelling of alcohols within the UAMI-EW model [4] is quite satisfactory for the description of properties of MeOH, EtOH and PrOH (1-propanol) in sufficiently large interval of pressures and of temperature. The present work complements our recent findings concerning this specific modelling [5, 29, 43]. Several properties, such as density, excess mixing volume, excess mixing enthalpy, static dielectric constant, surface tension, self-diffusion coefficients, all of them were critically evaluated and compared with available experimental data in detail. Some issues concerned the trends of behavior of a microscopic structure were elucidated as well [29, 43]. In addition, some insights about the changes of the cooperative features of hydrogen bonding in methanol upon high pressures have been discussed [6].

Rather than enumerating the findings of the present work, we prefer to focus on important extensions necessary to deal with. The first of them in our opinion is to investigate the models left out of attention for the moment. Namely, a set of more complex alcohols (e.g., the 2-propanol, 1- and 2-butanol, see SI of reference [4]) should be investigated on the same ground as simpler alcohols of the present study. Then, one can attempt to explore mixtures of primary alcohols, as well as mixtures of primary and secondary alcohols, similarly to reference [2]. Aqueous solutions of such models are necessary to study as well. Temperature and pressure dependence, besides the composition changes, of various properties should be explored. As regards the missing properties necessary to explore, we would like just to mention the shear viscosity and dielectric relaxation. Moreover, it is interesting to provide a more detailed description of interfacial phenomena beyond the surface tension. We expect that our simulation findings would stimulate the experimental measurements. Moreover, we expect progress of studies of microscopic structure of alcohols and their mixtures at high pressures using diffraction techniques, similarly to [6]. At the same time, one may attempt to refine a more sophisticated all-atom type models for alcohols and to intend the application of polarizable models.

References

1. Mathias P. M., *Ind. Eng. Chem. Res.*, 2019, **58**, 12465, doi:10.1021/acs.iecr.9b01624.
2. Chang Ch.-K., Siepmann J. I., *J. Chem. Eng. Data*, 2024, **69**, 509, doi:10.1021/acs.jced.3c00415.
3. Chen B., Potoff J. J., Siepmann J. I., *J. Phys. Chem. B*, 2001, **105**, 3093, doi:10.1021/jp003882x.
4. García-Melgarejo V., Núñez-Rojas E., Alejandre J., *J. Mol. Liq.*, 2021, **323**, 114576, doi:10.1016/j.molliq.2020.114576.
5. Aguilar M., Pusztai L., Pizio O., *Condens. Matter Phys.*, 2026, **29**, No. 1, 13502, doi:10.5488/CMP.29.13502.
6. Bakó I., Pusztai L., Pizio O., *J. Chem. Phys.*, 2025, **163**, 194504, doi:10.1063/5.0300069.
7. Gonzalez-Salgado D., Vega C., *J. Chem. Phys.*, 2016, **145**, 034508, doi:10.1063/1.4958320.
8. Ball P., *Life's Matrix: A Biography of Water*, Farrar, Straus, and Giroux, New York, 1999.
9. Franks F., *Water: A Matrix of Life*, Royal Society of Chemistry, Cambridge, 2000.
10. Vrhovšek A., Gereben O., Jamnik A., Pusztai L., *J. Phys. Chem. B*, 2011, **115**, 13473, doi:10.1021/jp206665w.

11. Weitkamp T., Neufeind J., Fischer H. E., Zeidler M. D., *Mol. Phys.*, 2000, **98**, 125, doi:10.1080/00268970009483276.
12. Spoel D., Lindahl E., Hess B., Groenhof G., Mark A. E., Berendsen H. J. C., *J. Comput. Chem.*, 2005, **118**, 1701, doi:10.1002/jcc.20291.
13. Linstrom P. J., Mallard W. G. (Eds.), *NIST Chemistry WebBook*, NIST Standard Reference Database 69, National Institute of Standards and Technology, Gaithersburg MD, 2025, doi:10.18434/T4D303.
14. Coquelet Ch., Valtz A., Richon D., de la Fuente J. C., *Fluid Phase Equilib.*, 2007, **259**, 33, doi:10.1016/j.fluid.2007.04.030.
15. Sun T. F., Schouten J. A., Trappeniers N. J., Biswas S. N., *J. Chem. Thermodyn.*, 1988, **20**, 1089, doi:10.1016/0021-9614(88)90115-2.
16. Moreau A., Sobrino M., Zambrano J., Segovia J. J., Villamañan M. A., Martín M. C., *J. Mol. Liq.*, 2021, **344**, 117744, doi:10.1016/j.molliq.2021.117744.
17. Neumann M., *Mol. Phys.*, 1983, **50**, 841, doi:10.1080/00268978300102721.
18. Bezman R. D., Casassa E. F., Kay R. L., *J. Mol. Liq.*, 1997, **73-74**, 397, doi:10.1016/S0167-7322(97)00082-2.
19. Dannhauser W., Bahe L. W., *J. Chem. Phys.*, 1964, **40**, 3058, doi:10.1063/1.1724948.
20. Davidson D. W., *Can. J. Chem.*, 1957, **35**, 458, doi:10.1139/v57-066.
21. Uosaki Y., Ito K., Kondo M., Kitaura S., Moriyoshi T., *J. Chem. Eng. Data*, 2006, **51**, 1915, doi:10.1021/je060248p.
22. Strey R., Schmeling T., *Ber. Bunsen Ges. Phys. Chem.*, 1983, **87**, 324, doi:10.1002/bbpc.19830870411.
23. Součková M., Klomfar J., Pátek J., *J. Chem. Eng. Data*, 2008, **53**, 2233, doi:10.1021/je8003468.
24. Vázquez G., Alvarez E., Navaza J. M., *J. Chem. Eng. Data*, 1995, **40**, 611, doi:10.1021/je00019a016.
25. Hurle R. L., Eastale A. J., Woolf L. A., *J. Chem. Soc., Faraday Trans. 1*, 1985, **81**, 769, doi:10.1039/F19858100769.
26. Karger N., Vardag T., Lüdemann H.-D., *J. Chem. Phys.*, 1990, **93**, 3437, doi:10.1063/1.458825.
27. Pratt K. C., Wakeham W. A., *J. Chem. Soc., Faraday Trans. 2*, 1977, **73**, 997, doi:10.1039/F29777300997.
28. Shaker-Gaafar N., Karger N., Wappmann S., Lüdemann H.-D., *Ber. Bunsen Ges. Phys. Chem.*, 1993, **97**, 805, doi:10.1002/bbpc.19930970610.
29. Mendez-Bermudez J. G., Pizio O., *J. Mol. Liq.*, 2025, **421**, 126789, doi:10.1016/j.molliq.2024.126789.
30. Wensink E. J. W., Hoffmann A. C., van Maaren P. J., van der Spoel D., *J. Chem. Phys.*, 2003, **119**, 7308, doi:10.1063/1.1607918.
31. Anisimov V. M., Vorobyov I. V., Roux B., MacKerell A. D., *J. Chem. Theory Comput.*, 2007, **3**, 1927, doi:10.1021/ct700100a.
32. Madhurima V., Ajmal Rahman M. K., Saishree K., Abdulkareem U., *Phys. Chem. Liq.*, 2024, **62**, 9, doi:10.1080/00319104.2023.2263897.
33. Lone B., Madhurima V., *J. Mol. Model.*, 2011, **17**, 709, doi:10.1007/s00894-010-0772-y.
34. Kumagai A., Yokoyama C., *Int. J. Thermophys.*, 1998, **19**, 3, doi:10.1023/A:1021438800094.
35. Boruń A., Žurada M., Bald A., *J. Therm. Anal. Calorim.*, 2010, **100**, 707, doi:10.1007/s10973-009-0157-6.
36. Mikhail S. Z., Kimel W. R., *J. Chem. Eng. Data*, 1961, **6**, 533, doi:10.1021/je60011a015.
37. Mikhail S. Z., Kimel W. R., *J. Chem. Eng. Data*, 1963, **8**, 323, doi:10.1021/je60018a014.
38. Benson G. C., Pflug H. D., *J. Chem. Eng. Data*, 1970, **15**, 382, doi:10.1021/je60046a020.
39. Iglesias M., Orge B., Tojo J., *J. Chem. Eng. Data*, 1996, **41**, 218, doi:10.1021/je950186v.
40. Torres R. B., Marchiore A., Volpe P., *J. Chem. Thermodyn.*, 2006, **38**, 526, doi:10.1016/j.jct.2005.07.012.
41. Lama R. F., Lu B. C.-Y., *J. Chem. Eng. Data*, 1965, **10**, 216, doi:10.1021/je60026a003.
42. Tomaszkiwicz I., Randzio S. L., Gierycz P., *Thermochim. Acta*, 1986, **103**, 281, doi:10.1016/0040-6031(86)85164-4.
43. Cruz Sanchez M., Trejos Montoya V., Pizio O., *Condens. Matter Phys.*, 2025, **28**, 13602, doi:10.5488/CMP.28.13602.
44. Marongiu B., Ferino I., Monaci R., Solinas V., Torrazza S., *J. Mol. Liq.*, 1984, **28**, 229, doi:10.1016/0167-7322(84)80027-6.
45. Tsvetov N., Sadaeva A., Toikka M., Zvereva I., Toikka A., *J. Therm. Anal. Calorim.*, 2020, **142**, 1977, doi:10.1007/s10973-020-09605-y.
46. Khurma J. R., Fenby D. V., *J. Phys. Chem.*, 1979, **83**, 2443, doi:10.1021/j100482a004.
47. Pflug H. D., Pope A. E., Benson G. C., *J. Chem. Eng. Data*, 1968, **13**, 408, doi:10.1021/je60038a032.
48. Galicia-Andrés E., Dominguez H., Pusztai L., Pizio O., *J. Mol. Liq.*, 2015, **212**, 70, doi:10.1016/j.molliq.2015.08.061.
49. Chmielewska A., Žurada M., Klimaszewski K., Bald A., *J. Chem. Eng. Data*, 2009, **54**, 801, doi:10.1021/je800593p.
50. Eudaira H., *Inorg. Chim. Acta*, 1980, **40**, X104, doi:10.1016/S0020-1693(00)92195-9.

51. Golubev V. A., J. Mol. Liq., 2024, **414**, 126266, doi:10.1016/j.molliq.2024.126266.

II. Температурна залежність властивостей простих одноводневих спиртів. Молекулярно-динамічне моделювання моделі UAMI-EW об'єднаного атома

М. Агілар¹, Е. Нуньєс-Рохас², О. Пізіо¹

¹ Інститут хімії, Національний автономний університет Мексики, Сіркуіто Екстеріор, 04510, Мексика

² Факультет хімії, Столичний автономний університет Ітапалапа, просп. Сан Рафаель Атілско 186, Віцентіна, 09340, Мехіко, Мексика

З використанням ізобарно-ізотермічного комп'ютерного моделювання молекулярної динаміки досліджується залежність від температури низки властивостей простих одноводневих спиртів. Зокрема, досліджуються метанольний (MeOH), етанольний (EtOH) та 1-пропаноловий (PrOH) спирти. З цією метою для кожного зі спиртів застосовується нещодавно запропоноване неполяризоване силове поле об'єднаного атома [V. García-Melgarejo et al., J. Mol. Liq., 2021, **323**, 114576]. Точність силового поля обговорюється шляхом порівняння прогнозів моделювання та експериментальних даних для густини, діелектричної проникності, поверхневого натягу, та коефіцієнта самодифузії. Додаткові дані щодо застосовності моделі отримані шляхом дослідження залежності різних властивостей від складу сумішей MeOH-PrOH. З'ясовано особливості змішування частинок у цій системі з точки зору густини, надлишкового об'єму змішування та надлишкової ентальпії змішування. Отримано статичну діелектричну проникність суміші та відповідний надлишок. Наприкінці статті прокоментовано перспективи моделювання.

Ключові слова: метанол, етанол, 1-пропанол, температурна залежність, молекулярно-динамічне моделювання
